

## Optimized graph-based segmentation for ultrasound images



Qinghua Huang<sup>a,\*</sup>, Xiao Bai<sup>b</sup>, Yingguang Li<sup>a</sup>, Lianwen Jin<sup>a</sup>, Xuelong Li<sup>c</sup>

<sup>a</sup> School of Electronic and Information Engineering, South China University of Technology, Guangzhou 510641 Guangdong, PR China

<sup>b</sup> School of Computer Science and Engineering, Beihang University, Beijing 100191, PR China

<sup>c</sup> Center for OPTical IMagery Analysis and Learning (OPTIMAL), State Key Laboratory of Transient Optics and Photonics, Xi'an Institute of Optics and Precision Mechanics, Chinese Academy of Sciences, Xi'an 710119, Shaanxi, PR China

### ARTICLE INFO

#### Article history:

Received 8 May 2013

Received in revised form

3 August 2013

Accepted 14 September 2013

Communicated by Mingli Song

Available online 24 October 2013

#### Keywords:

Evolutionary learning

Ultrasound image segmentation

Particle swarm optimization

Graph theory

### ABSTRACT

Segmentation of medical images is an inevitable image processing step for computer-aided diagnosis. Due to complex acoustic inferences and artifacts, accurate extraction of breast lesions in ultrasound images remains a challenge. Although there have been many segmentation techniques proposed, the performance often varies with different image data, leading to poor adaptability in real applications. Intelligent computing techniques for adaptively learning the boundaries of image objects are preferred. This paper focuses on optimization of a previously documented method called robust graph-based (RGB) segmentation algorithm to extract breast tumors in ultrasound images more adaptively and accurately. A novel technique named as parameter-automatically optimized robust graph-based (PAORGB) image segmentation method is accordingly proposed and performed on breast ultrasound images. A particle swarm optimization algorithm is incorporated with the RGB method to achieve optimal or approximately optimal parameters. Experimental results have shown that the proposed technique can more accurately segment lesions from ultrasound images compared to the RGB and two conventional region-based methods.

© 2013 Elsevier B.V. All rights reserved.

### 1. Introduction

Breast cancer is one of the most deadly cancers in women. Because it is relatively inexpensive, noninvasive and accurate, medical ultrasound (US) imaging has been regarded as one of the gold standards for breast tumor diagnosis [1]. Early detection of cancerous lesions is crucial for successful treatment and cure of breast cancer. However, there are many speckles and shadows in US images, which make the diagnoses subject to the radiologist's experience and skills. As a second reader, computer-aided diagnosis (CAD) can largely increase the efficiency and effectiveness of breast cancer screening. In CAD systems, segmentation of lesions is the most essential and important step for further tumor analysis [2].

There have been many segmentation methods proposed for various applications, e.g. computer vision [3], object recognition [4–6], and medical imaging [3,4,7–9]. Some of the methods have been focusing on breast ultrasound (BUS) images [1,10–15]. Most of the conventional methods can be grouped into two categories, i.e. the clustering and the active contour model (ACM). Clustering which is an unsupervised learning method uses an iterative

method to find clustering centers according to a criterion that minimize the squared distances between sample points and the clustering centers. The main strength of clustering based method is that it can be automatically performed without the need to set the initial contour. Xu and Nishimura [11] proposed a method which uses the Fuzzy C-Means (FCM) which is a clustering method incorporating both intensity and texture information of images to extract breast lesions in US images. The method is more tolerant to noises than conventional FCM, but the parameters in the method are manually assigned, leading to unstable segmentation results.

The ACM also called snake is another popular segmentation method for US images. It deforms in an iterative manner to be close to the contour of breast tumor. The main weakness of this method is that its segmentation results heavily depend on the initial definition of object contours. The segmentation results would be inaccurate if initial contours are poorly defined. Currently, the initial contours in the ACM methods can be defined by either manual delineations or some complexly auto-initialized methods. However, it is not easy to find out an automatic scheme for defining the initial contours because of the blurry boundaries inherent in the US images. Huang and Chen [12] utilized the watershed transform and the ACM to overcome the natural properties of US images, i.e. speckles and noises. In this method, the watershed transform is treated as the automatic initial contouring procedure to maintain a rough tumor shape for the ACM.

\* Corresponding author. Tel.: +86 20 87113540.

E-mail addresses: [qhhuang@scut.edu.cn](mailto:qhhuang@scut.edu.cn) (Q. Huang), [baixiao@buaa.edu.cn](mailto:baixiao@buaa.edu.cn) (X. Bai), [yingguangli@126.com](mailto:yingguangli@126.com) (Y. Li), [eelwj@scut.edu.cn](mailto:eelwj@scut.edu.cn) (L. Jin), [xuelong\\_li@opt.ac.cn](mailto:xuelong_li@opt.ac.cn) (X. Li).

However, its performance varies with different images. Madabhushi and Metaxas [13] presented a technique to automatically find lesion margins in US images. They used a method that combines intensity and texture along with directional gradient to roughly define the initial contours of breast lesions before using the ACM. Nevertheless, there are several parameters that should be carefully assigned in the method. In order to obtain good segmentation results, the parameters should be manually adjusted with respect to different US images.

In addition to the clustering and ACM methods, graph-based segmentation techniques have become a hot research topic due to their simple structure and solid theories [16,17]. Taking advantage of graph theory, a graph-based image segmentation method aims to make the neighboring pixels having similar intensities into one minimal spanning tree (MST), which corresponds to a region of the image. Huang et al. [14] proposed a method called robust graph-based (RGB) method based on the graph theory and firstly applied it for segmenting breast tumors in US images. In that study, two significant parameters in graph-based segmentation algorithm were empirically selected to achieve relatively good results.

Generally speaking, there are one or more parameters that are crucial to the final results in most of previously reported segmentation methods. However, the parameters are usually manually assigned by repeatedly testing to achieve acceptable results. Therefore, how to find out the optimal or approximately optimal values for the parameters using an optimization method is worth being investigated.

In this study, we focus on incorporating an optimization method into a previously reported segmentation method, i.e. the RGB method [14], because the RGB is a typical segmentation method whose performance heavily relies on the parameter settings. The optimal or approximately optimal parameters can be found in the hybrid scheme which is finally evaluated using a set of BUS images. Many popular evolutionary learning algorithms [18–23] are capable of solving global optimization problems. In this study, the particle swarm optimization (PSO) algorithm is chosen for finding the optimal parameters in the RGB and the PSO algorithm not only shares many advantages with evolutionary computing algorithms but also possesses improved computational efficiency.

This paper is organized as follows. Section 2 introduces the proposed parameter-automatically optimized robust graph-based segmentation method (called PAORGB segmentation method) for breast tumors in US images. A brief description of the RGB segmentation method, evaluation function for optimization, the standard particle swarm optimization algorithm and the proposed method are given. Section 3 presents and discusses the experimental results of the proposed method with a systematic comparison with those produced by the RGB with the parameters

empirically selected, an automatic segmentation method [13], conventional K-means and FCM clustering algorithms. In Section 4, we finally draw the conclusions for this study.

## 2. Methods

In this study, we propose to incorporate a PSO algorithm into the RGB segmentation method to optimize the parameters, so as to make the results of the RGB method more reliable and accurate for segmenting breast tumors in US images. The RGB method, evaluation function for optimization and the PSO algorithm are firstly briefly introduced, and the proposed hybrid approach is thereafter described and summarized.

### 2.1. Robust graph-based segmentation method

Before the implementation of the RGB, a speckle reduction procedure is needed to improve the quality of US images, because there are plenty of artifacts (e.g. attenuations, speckles, shadow and signal dropout) in US images [24]. Bilateral filter which has been proved to be an efficient and effective method for speckle reduction is firstly used in this study. Readers may refer to [25] for more technical details. Fig. 1 shows the performance of the bilateral filter.

Given an image which is initially regarded as a graph, the RGB method aims to merge spatially neighboring pixels which are of similar intensities into a minimal spanning tree (MST), which corresponds to a subgraph (i.e. a subregion of the image). The image can therefore be grouped into several subregions (i.e. a forest of MST). Obviously, the step for mergence of pixels into a MST is the key, determining the final segmentation results. In [14], we previously proposed a pairwise region comparison predicate to determine whether or not a boundary between two subgraphs should be eliminated. Given a graph  $G=(V,E)$ , the resulting predicate  $D(C_1,C_2)$  which compares the inter-subgraph differences to the within subgraph differences is expressed by

$$D(C_1,C_2) = \begin{cases} \text{true} & \text{if } Dif(C_1,C_2) > MInt(C_1,C_2) \\ \text{false} & \text{other} \end{cases} \quad (1)$$

$$Dif(C_1,C_2) = |\mu(C_1) - \mu(C_2)| \quad (2)$$

$$MInt(C_1,C_2) = \min(\sigma(C_1) + \tau(C_1), \sigma(C_2) + \tau(C_2)) \quad (3)$$

$$\tau(C) = \frac{k}{|C|} \cdot \left(1 + \frac{1}{\alpha \cdot \beta}\right), \quad \beta = \frac{\mu(C)}{\sigma(C)} \quad (4)$$

where  $Dif(C_1,C_2)$  is the difference between two subgraphs,  $C_1$  and  $C_2 \in V$ ,  $MInt(C_1,C_2)$  represents the smallest internal difference of  $C_1$  and  $C_2$ ,  $\mu(C)$  denotes the average intensity of  $C$ ,  $\sigma(C)$  is the

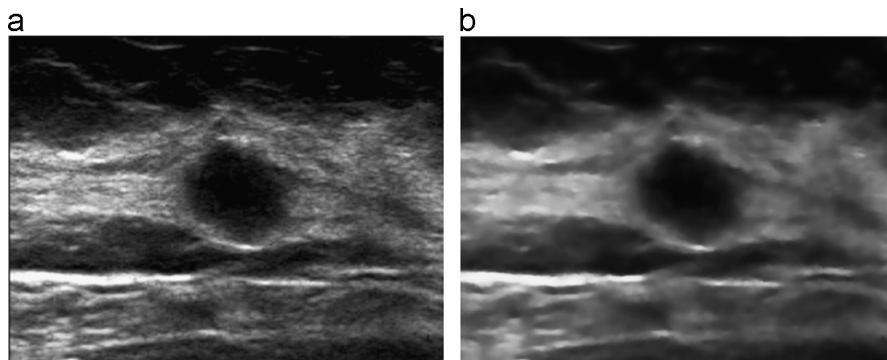


Fig. 1. An illustration of the bilateral filter's performance. (a) Original image, and (b) filtered image.

standard deviation of  $C$ ,  $\tau(C)$  is a threshold function of  $C$ ,  $\alpha$  and  $k$  are positive parameters.

Based on the pairwise region comparison predicate, the summarized procedures for segmentation of an image are as the following.

*Step 1:* Construct a graph  $G=(V,E)$  for a US image. In  $G$ , each pixel corresponds to a vertex and an edge connects two spatially neighboring vertices. The edge weight is defined by absolute intensity difference between two adjacent pixels. Initially, each vertex can be regarded as a subgraph and all of the edges forming an edge set  $E$  are valid.

*Step 2:* Sort the edges in  $E$  in non-descending order in terms of the edge weight. Set  $q=1$ .

*Step 3:* Pick the  $q$ th edge in the sorted edges. If the  $q$ th edge is a valid edge (i.e. it connects two different subgraphs) and the boundary between the two subgraphs can be eliminated with respect to the pairwise region comparison predicate as mathematically expressed in Eqs. (1)–(4), the two subgraphs are merged into a larger subgraph and this edge is set to be invalid.

*Step 4:* Let  $q=q+1$ . Repeat Step 3 until all edges in  $E$  have been traversed.

When all edges have been traversed, a forest including a number of MSTs can be obtained. Each MST corresponds to a subregion in the image. Apparently, the selections of  $\alpha$  and  $k$  in the predicate introduced above would significantly influence the segmentation results. In [14], the two parameters were empirically selected. However, due to various appearances of BUS images, fixed settings for the two parameters in the RGB may not lead to acceptable segmentation performance for any of BUS images. Therefore, an optimization scheme for the parameter setting in the RGB is required to automatically select optimal or approximately optimal parameters for a specific BUS image in order to achieve the most acceptable segmentation result. In this study, we are aiming to find appropriate  $\alpha$  and  $k$  using the PSO algorithm.

## 2.2. Objective function for parameter optimization

Prior to the implementation of the PSO algorithm to find out appropriate parameters in the RGB, an objective function should be determined. A well designed objective function can make an optimization method find the optimal solutions in a rapid and efficient manner.

Due to the relatively low quality of clinical BUS images, a good segmentation method has to make use of task-specific constraints or priors [24] to improve the final results. In this study, we first ask the operator to roughly delineate a small rectangular region in which the breast lesion of interest is fully contained and located at the central part, and to extract this region from the original BUS

image. By this way, the interferences from other regions unrelated to the lesions of interest can be reduced as much as possible. Such a small image is called tumor centered image (TCI) in this study. Fig. 2 shows how a TCI is extracted from an original BUS image. It is worth noting that a TCI is visually found and manually delineated by an operator. Therefore, the operator must be experienced in accurately finding a lesion of interest.

We apply the RGB method to the TCI in this study. When the TCI is divided into several subregions, it is assumed that the central subregion (including the central pixel) should contain most part of the lesion because we have an a priori that the lesion is locating at the central part of the TCI. Thus, the central subregion is regarded as the *reference region*. The reference region is defined as the subregion that contains the central pixel of the TCI in the segmentation result of the RGB method. Fig. 3 gives an example of the reference region. Reference region varies with the selection of  $\alpha$  and  $k$ . If the values of  $\alpha$  and  $k$  are optimally or approximately optimally selected, the reference region equals the breast tumor subregion.

Because the reference region corresponds to the lesion in a BUS image, our objective is to maximize the difference between the reference region and its surrounding subregions. We take advantage of a notion called Otsu's method [26] which can overcome the problems of over- and under-segmentation. It selects an optimum threshold by maximizing the between-class variance in a gray image. Inspired by Otsu's method, the objective function  $S_B$  for this study is defined below:

$$S_B = \sum_{i=0}^{n-1} P(C_i)(\mu(C_i) - \mu(C_{Ref}))^2 \quad (5)$$

where  $n$  denotes the number of the subregions adjacent to the Reference Region,  $\mu(C)$  denotes the mean intensity of subregion  $C$  and  $P(C_i)$  denotes the proportion of subregion  $C_i$  among all of the  $n$  subregions in the TCI, expressed as

$$P(C_i) = \frac{|C_i|}{\sum_{i=0}^{n-1} |C_i|} \quad (6)$$

where  $|C|$  is the size of subregion  $C$ .

It can be obviously concluded that the largest  $S_B$  corresponds to the maximal difference between the reference region and its surrounding regions. With the proposed objective function, we choose the PSO algorithm to be the optimization method used to improve the performance of the RGB.

## 2.3. Particle swarm optimization algorithm

Particle swarm optimization (PSO) algorithm is an evolutionary computation technique mimicking the behavior of flying birds and

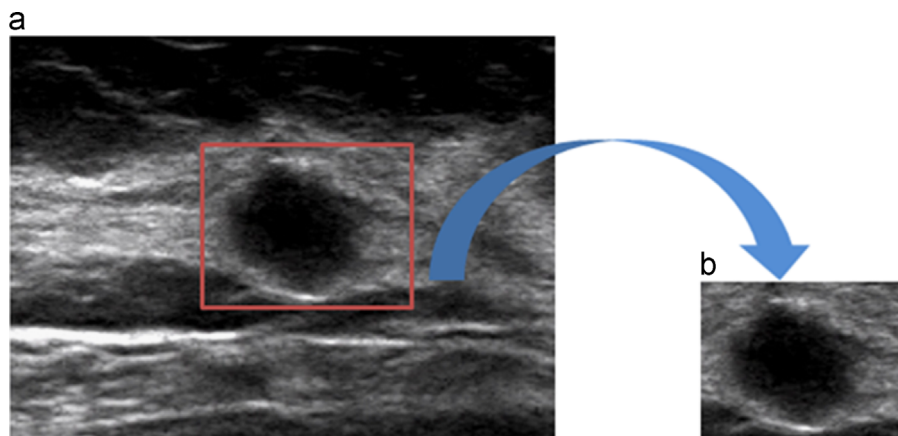
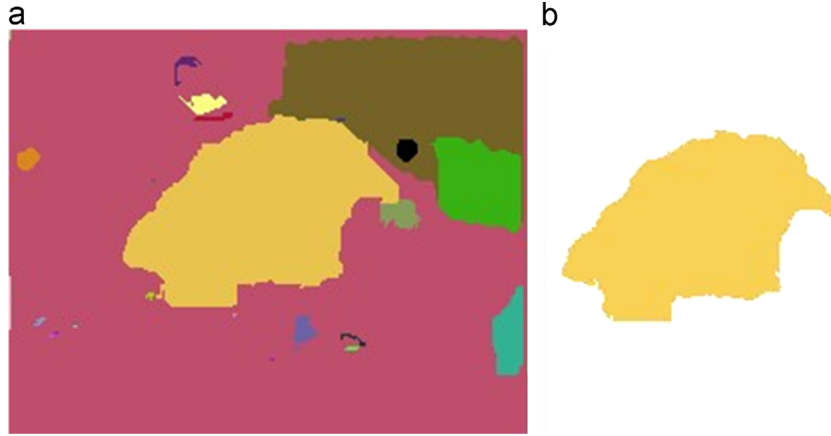


Fig. 2. Roughly delineate the tumor centered image. (a) An original BUS image, and (b) tumor centered image cut from (a).



**Fig. 3.** The illustration of the reference region. (a) A segmented image by the RGB, and (b) the reference region of (a).

their means of information exchange [17]. In the PSO algorithm, each particle represents a potential solution, and the particle swarm is initialized with a population of random individuals in the search space. The algorithm searches the optimal solution by updating the positions of the particles in an evolutionary manner.

Supposing there are  $n_p$  solutions each of which corresponds to a particle, the position (i.e. the solution) and velocity of the  $i$ th particle,  $i = 1, \dots, n_p$ , is represented by two  $m$ -dimensional vectors, i.e.  $x_i = (x_{i1}, x_{i2}, \dots, x_{im})$  and  $v_i = (v_{i1}, v_{i2}, \dots, v_{im})$ , respectively. According to the specific issues, an objective function is used to evaluate the fitness of each particle. The best position of the  $i$ th particle  $p_i = (p_{i1}, p_{i2}, \dots, p_{im})$  is the best preciously visited position of the  $i$ th particle during the updating process. The global best position of the whole swarm obtained so far is indicated as  $p_g = (p_{g1}, p_{g2}, \dots, p_{gm})$ . At each generation, every particle tries to modify its position according to the current velocity,  $p_i$  and  $p_g$ . The velocity  $v_i^{t+1}$  of each particle and its new position  $x_i^{t+1}$  are updated according to the following equations:

$$v_i^{t+1} = wv_i^t + c_1r_1(p_i^t - x_i^t) + c_2r_2(p_g^t - x_i^t) \quad (7)$$

$$x_i^{t+1} = x_i^t + v_i^{t+1} \quad (8)$$

where  $t$  is the generation number,  $w$  is the inertia weight,  $c_1$  and  $c_2$  are positive parameters known as acceleration coefficients, determining the relative influence of the cognition and social components, and  $r_1$  and  $r_2$  are independently uniformly distributed random variables in the range of (0, 1). In the equation,  $wv_i^t$  represents the influence of the previous velocity of particle on its current one.  $c_1r_1(p_i^t - x_i^t)$  represents the personal experience.  $c_2r_2(p_g^t - x_i^t)$  represents the collaborative effect of the particles and it always pulls the particle to the global best solution that the swarm has found so far.

At each generation, the velocity of each particle is calculated according to Eq. (7), and the position is updated by using Eq. (8). Each time, any better position is stored for the next generation. Each particle adjusts its position by its own ‘flying’ experience and the experience of its companions. This means that if a particle arrives at a promising new position, all the other particles will move closer to it. This process is repeated until satisfactory solution is found or a predefined number of generation is met.

The detailed procedures are summarized as follows:

*Step 1:* According to the search space, properly set the population size and randomly initialize the particles.

*Step 2:* Iteratively traverse all the particles.

*Step 3:* In each traverse, evaluate every particle based on a predefined objective function and update its position according to Eqs. (7) and (8).

*Step 4:* Repeat Step 3 until all particles’ positions have been converged to an acceptable extent or the iterative number has reached the predefined.

#### 2.4. The proposed image segmentation method

As mentioned above, the values of parameters  $\alpha$  and  $k$  can greatly influence the performance of the RGB algorithm. Proper setting of  $\alpha$  and  $k$  leads to acceptable segmentation results. By taking advantage of the PSO algorithm and the objective function designed in this study, we propose a new method that is called parameter-automatically optimized robust graph-based (PAORGB) image segmentation algorithm. Generally speaking, the PAORGB segmentation method combines a segmentation method (i.e. the RGB) and an optimization method (i.e. the PSO). In each generation, every particle completes the RGB segmentation method for a given BUS image and the objective function is used to evaluate this particle and update the two parameters (i.e.  $\alpha$  and  $k$ ) in the RGB for improving the segmentation performance in the next generation. The position and velocity of a particle are expressed as  $x_i = (k_i, \alpha_i)$  and  $v_i = (v_{ki}, v_{\alpha i})$ , respectively.

The PAORGB method is summarized as the following.

*Step 1:* Manually delineate the TCI from the original US breast tumor image.

*Step 2:* Use the bilateral filter to reduce the speckles in the image.

*Step 3:* Set the population size  $n_p$  and randomly initialize the particles in the search space.

*Step 4:* Iteratively traverse all the particles. Let  $q = 1$ .

*Step 5:* In the  $q$ th traversal, for each particle, we use its position, i.e.  $x_i = (k_i, \alpha_i)$ , to execute the RGB segmentation algorithm. Based on the evaluation function (i.e. Eq. (5)) in Section 2.2, the segmentation result is evaluated and the particle’s position is updated according to Eqs. (7) and (8) in section IIC.

*Step 6:* Repeat Step 4 until all particles have been converged to a certain condition (i.e. the updating of  $k$  is below 1 and that of  $\alpha$  is below 0.00001 for all the particles in an experiment) or  $q = N$ , where  $N$  is the predefined maximum number of generations.

When the iteration process is over, the global best particle position corresponds to the optimal or approximately optimal combination of  $\alpha$  and  $k$ . With the searched  $\alpha$  and  $k$ , we conduct the RGB method and achieve the final segmentation results. Fig. 4 shows the flow chart of the proposed PAORGB method.

#### 2.5. Experimental methods

According to our previous investigations [14], for segmenting breast tumor in US images,  $k$  varies from 1 to 4000 and  $\alpha$  from 0.0001 to 4.000, thus forming the search space of the PSO. After a

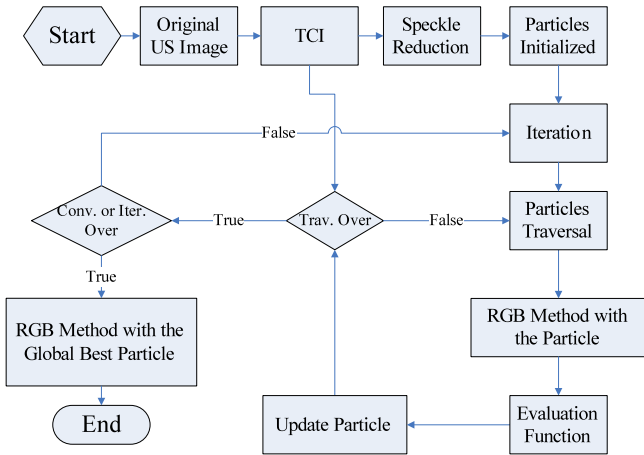


Fig. 4. The flowchart for the PAORGB method (Conv., convergence; Trav., traversal; Iter., iteration).

random initialization of the  $n_p$  ( $n_p=800$  in this study) particles, we use Eqs. (7) and (8) to update the positions and velocities of the particles in the PAORGB. As suggested in [19], we set  $w=1$ ,  $c_1=1$ , and  $c_2=1$  in this study. The maximum generation number  $N$  is empirically set to 1000.

The PAORGB method is developed using Visual C++ (Microsoft, USA) and runs on a CPU of 3.0 GHz and a RAM of 2 GB. We test the PAORGB method using 20 BUS images, 10 of which are benign tumors and the others of which are malignant. The images are provided by Medical School, Shenzhen University, China. To illustrate whether or not the parameters have been optimized, we test the images using the RGB method with suggested combinations of parameters  $\alpha$  and  $k$  [14] and make the comparisons with the proposed method. In addition, these images are tested using the K-means and the FCM methods which have been recognized as two efficient region based methods for image segmentation for comparison purpose. In the K-means and FCM methods, both  $K$  and  $c$  (i.e. the numbers of classes) are carefully set to make the target regions isolated from the backgrounds. Finally, the proposed method is compared with a fully automatic segmentation method (called Madabhushi's method in this paper) [13].

To quantitatively compare different segmentation methods, we use four criteria, i.e. averaged radial error (ARE), true positive volume fraction (TPVF), false positive volume fraction (FPVF) and false negative volume fraction (FNVF), to evaluate segmentation results. Averaged radial error (ARE) [14] is used for evaluation of segmentation performance by measuring average radial error of the contours, with respect to the real contours which are achieved by averaging the lesion boundaries delineated by three experienced radiologists. The ARE is defined as

$$ARE(n) = \frac{1}{n} \sum_{i=0}^{n-1} \frac{|Cs(i) - Cr(i)|}{|Cr(i) - C_0|} \times 100\% \quad (9)$$

where  $n$  indicates the number of radial rays and is set to be 180 in our experiments,  $C_0$  represents the center of the "true" tumor region which is delineated by experienced radiologists,  $C_s(i)$  denotes the location where the contour of the segmented tumor region is crossing the  $i$ th ray, and  $C_r(i)$  is the location where the contour of the "true" tumor region is crossing the  $i$ th ray. It is obvious that smaller ARE corresponds to better segmentation accuracy. Fig. 5 illustrates the computation principle for the ARE.

In addition, the TPVF, FPVF and FNVF are often used in evaluation of the performance of segmentation methods. The TPVF means true positive volume fraction, indicating the total fraction of tissue in the 'true' tumor region with which the segmented region overlapped. The FPVF means false positive volume fraction, denoting the

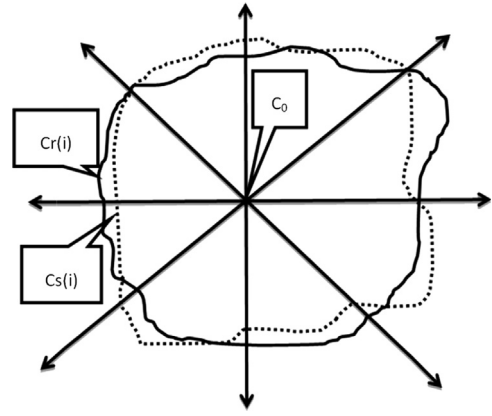


Fig. 5. An illustration of computation principle for the ARE.

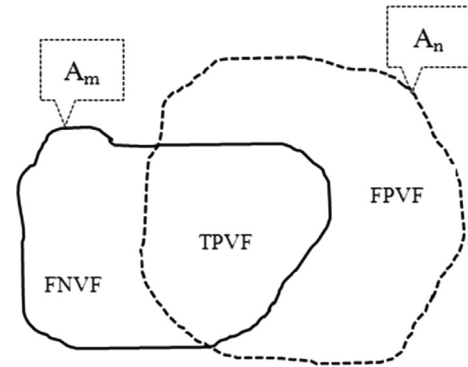
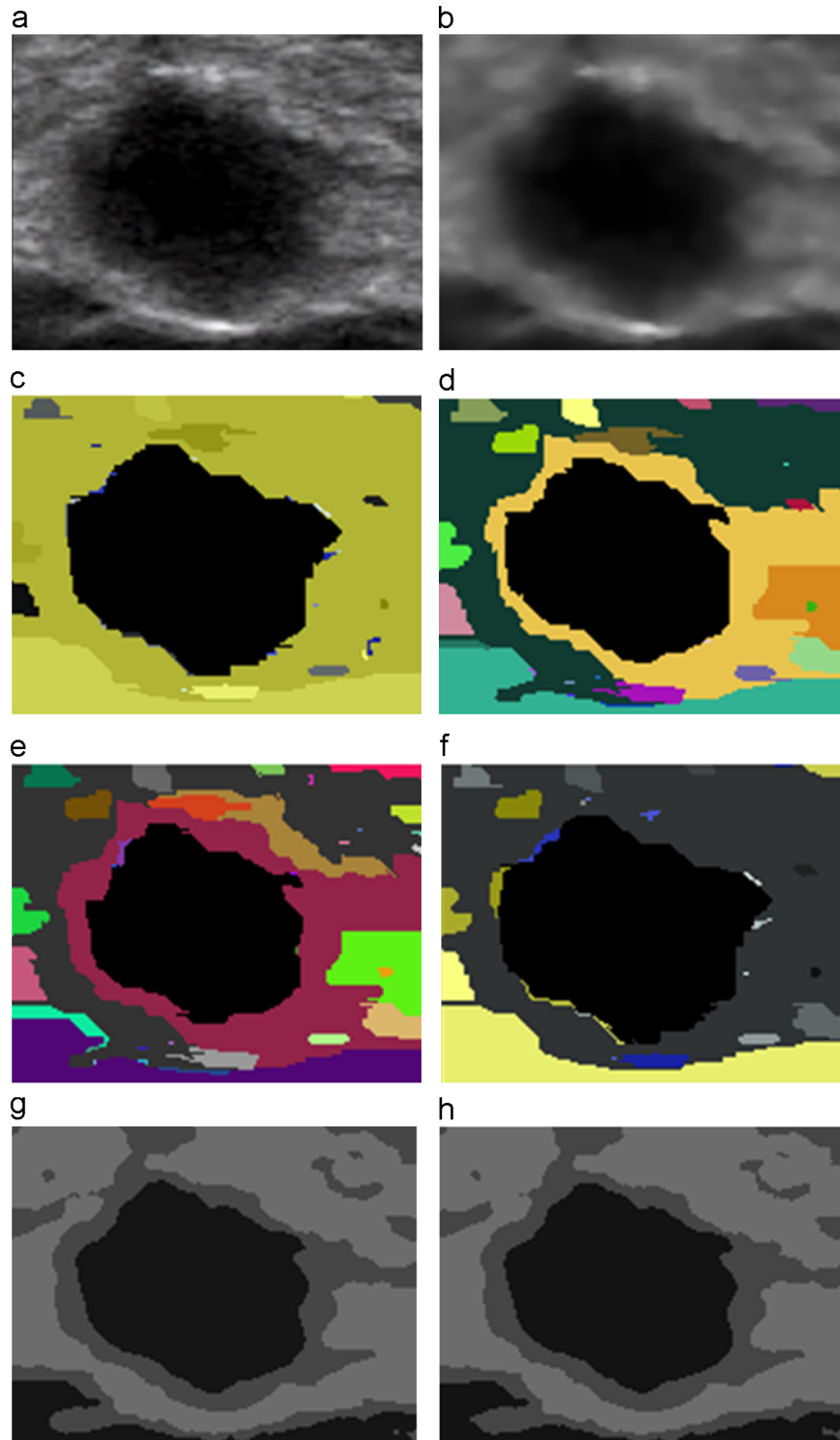


Fig. 6. The areas corresponding to TPVF, FPVF and FNVF, respectively.  $A_m$  indicates the 'true' contour delineated by radiologists and  $A_n$  denotes the contour computed using a segmentation algorithm.

amount of tissue falsely identified by the segmentation method as a fraction of the total amount of tissue in the 'true' tumor region. The FNVF means false negative volume fraction, denoting the fraction of tissue defined in the 'true' tumor region that was missed by a segmentation method. Therefore, larger TPVF, smaller FPVF and smaller FNVF indicate better segmentation performance. In this study, the 'true' tumor regions are determined by averaging the region boundaries delineated by the three radiologists. Fig. 6 shows the areas corresponding to the TPVF, FPVF and FNVF, respectively.

### 3. Experimental results

In the experiments, the evolution of the PAORGB terminates within 320 generations for each of the testing images, and takes 12.2 min on average, which is much longer than its counterparts. Figs. 7 and 8 demonstrate the segmentation results of a benign tumor and a malignant tumor, respectively, using different methods (i.e. the RGB with default parameters suggested in [14], the proposed PAORGB, the K-means and the FCM clustering methods). For breast tumor US images, the parameters  $k$  and  $\alpha$  are suggested to be 2000 and 0.01–0.05, respectively [14]. In this study, we set  $(k, \alpha)$  in the RGB to be (2000, 0.01), (2000, 0.02), and (2000, 0.03), respectively, and the resultant segmentations can be seen in Figs. 7c–e and 8c–e. It can be observed that the RGB with suggested parameters leads to an over-segmentation. Figs. 7f and 8f are the segmentation results of the proposed method, offering visually improved segmentation results in comparison with the RGB's results. The segmentation results using the K-means and the FCM clustering methods are also shown in Figs. 7g, h, 8g and h,



**Fig. 7.** Segmentation results of a benign tumor. (a) Source image, (b) filtered image, (c)  $k=2000$ ,  $\alpha=0.01$ , (d)  $k=2000$ ,  $\alpha=0.02$ , (e)  $k=2000$ ,  $\alpha=0.03$ , (f)  $k=355$ ,  $\alpha=0.002$ , (g) K-means,  $K=3$ , and (h) FCM,  $m=2$ ,  $C=3$ .

respectively. Visually, the proposed method also outperforms the K-means and FCM methods, especially for the malignant tumor as illustrated in Fig. 8.

When applying Madabhushi's method [13] to the testing images, it is only effective in 12 of the 20 testing BUS images because it cannot always correctly find the seed points for the tumors. When the seed for locating the lesion of interest is incorrectly found, a totally unacceptable segmentation is resulted in. Fig. 9 shows the comparison of segmentation results between the proposed method

and Madabhushi's method. The tumor contour curves of the PAORGB in Fig. 9 are the boundary of the reference regions which are the lesions of interest. It is obviously seen that the contours generated by the proposed PAORGB are visually smoother and more accurate than those delineated by Madabhushi's method.

Table 1 presents the quantitative comparisons of different segmentation methods based on the 20 breast US images. As mentioned above, quantitative results for the four measures for evaluation of segmentation performance are given in this table. Similarly, we

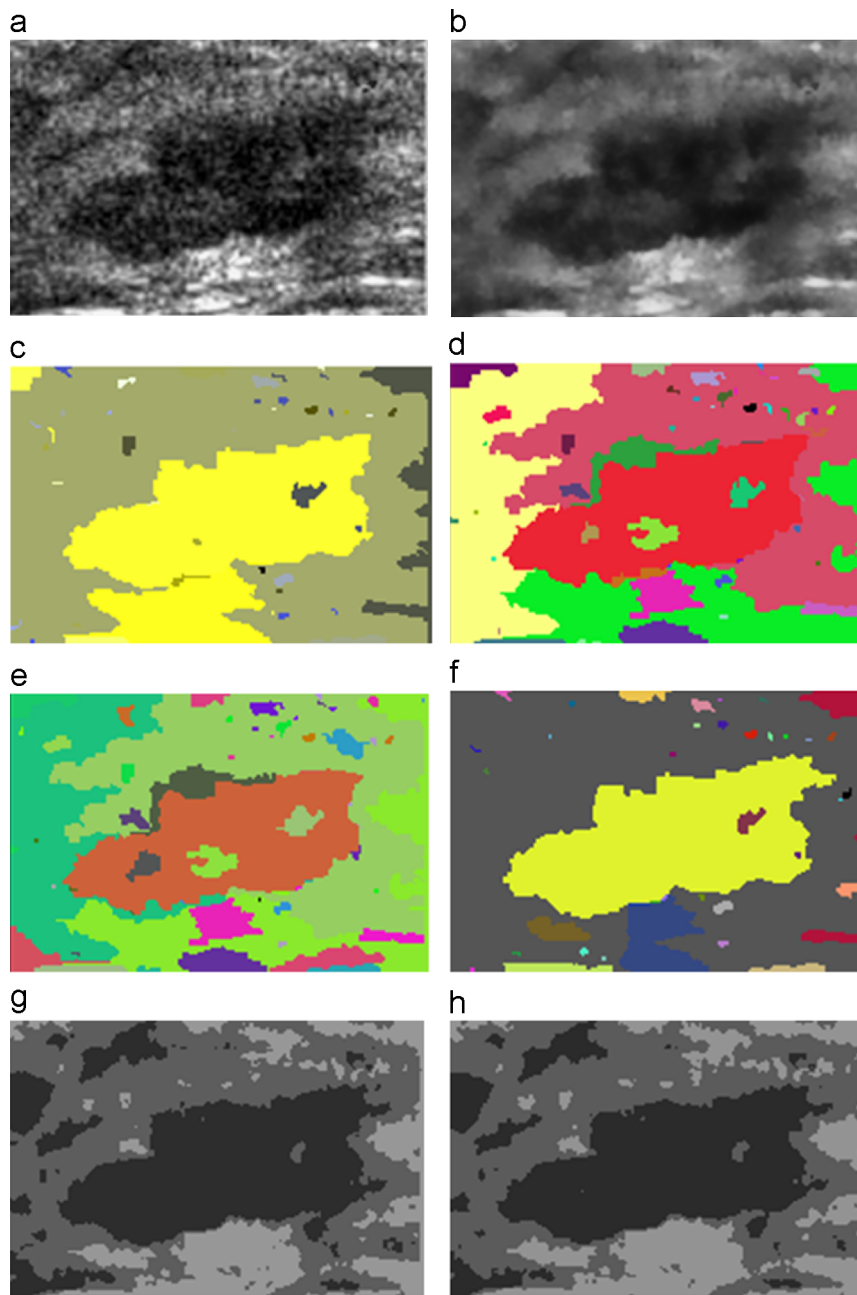


**Fig. 8.** Segmentation results of a malignant tumor. (a) Source image, (b) filtered image, (c)  $k=2000$ ,  $\alpha=0.01$ , (d)  $k=2000$ ,  $\alpha=0.02$ , (e)  $k=2000$ ,  $\alpha=0.03$ , (f)  $k=1175$ ,  $\alpha=0.0004$ , (g) K-means,  $K=3$ , and (h) FCM,  $m=2$ ,  $C=3$ .

present the evaluations of the benign and malignant tumors, respectively, as presented in Tables 2 and 3. It can be observed that the proposed PAORGB method outperforms the other methods for the ARE, TPVF and FNVF, and takes the second place for the FPVF, indicating a significant improvement of segmentation performance for the BUS images with either benign or malignant lesions. It is noted that all of the segmentation methods almost perform better on benign tumors, indicating that the boundaries of benign lesions are more significant than those of malignant lesions.

#### 4. Discussions and conclusions

This paper introduces a new segmentation method for segmenting breast tumors in US images. The proposed method is based on a previously reported graph-based segmentation

algorithm (i.e. the RGB) and incorporates a particle swarm optimization algorithm to optimize the parameters (i.e.  $k$  and  $\alpha$ ) in order to overcome the problems of under-segmentation or over-segmentation and improve the segmentation performance. By making use of between-class variance maximum theory (i.e. OTSU) to design the objective function of PSO, the proposed approach is able to find out the optimal or approximately optimal parameters for the RGB method within a limited computation period. The experimental results have demonstrated that the proposed PAORGB method significantly improves the performance of the RGB and outperforms a previously reported automatic segmentation algorithm and two conventionally used region based methods (i.e. the K-means and the FCM methods). Especially, the technical improvement of the PAORGB is more significant for the benign breast tumors according to Table 2, indicating good merit in real clinical applications.

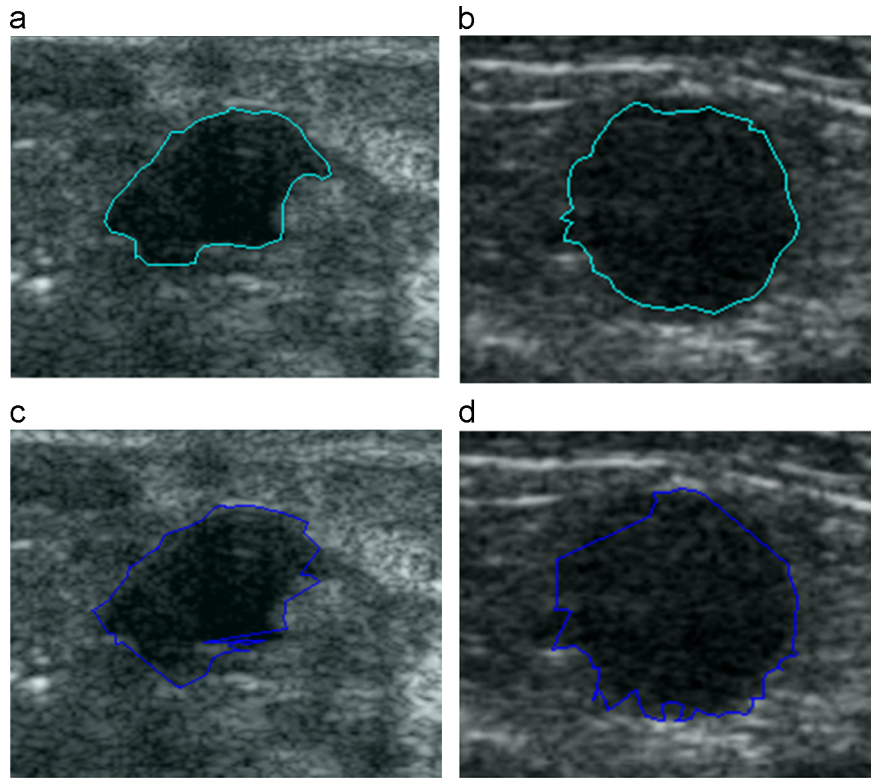


Fig. 9. Comparisons between the PAORGB and Madabhushi's method. (a,b) Segmentation results of the PAORGB, and (c,d) segmentation results of Madabhushi's method.

**Table 1**  
Overall segmentation performance (in percentage) of five segmentation methods (the best values are in bold).

Methods	ARE (%)	TPVF (%)	FPVF (%)	FNVF (%)
PAORGB	<b>7.0 ± 2.3</b>	<b>90.1 ± 4.3</b>	2.2 ± 0.9	<b>9.9 ± 4.3</b>
RGB ( $k = 2000, \alpha = 0.02$ )	10.3 ± 1.2	84.3 ± 8.1	<b>1.4 ± 1.4</b>	15.7 ± 8.2
K-means ( $K=3$ )	11.2 ± 2.7	83.8 ± 4.8	2.6 ± 2.5	16.2 ± 4.8
FCM ( $c=3$ )	18.2 ± 12.9	83.0 ± 5.2	3.2 ± 2.6	17.0 ± 5.3
Mad.'s method	14.1 ± 7.0	82.0 ± 11	8.3 ± 5.5	18.0 ± 11

**Table 2**  
Segmentation performance (in percentage) of the five segmentation methods on BUS images with benign tumors (the best values are in bold).

Methods	ARE (%)	TPVF (%)	FPVF (%)	FNVF (%)
PAORGB	<b>5.0 ± 1.0</b>	<b>93.3 ± 2.5</b>	2.7 ± 0.7	<b>6.7 ± 2.5</b>
RGB ( $k = 2000, \alpha = 0.02$ )	9.4 ± 2.2	85.8 ± 12	1.8 ± 1.1	14.2 ± 12
K-means ( $K=3$ )	10.7 ± 1.4	85.1 ± 3.2	3.5 ± 3.6	14.8 ± 3.2
FCM ( $c=3$ )	13.2 ± 3.4	85.3 ± 5.1	<b>1.0 ± 0.8</b>	20.6 ± 4.7
Mad.'s method	13.4 ± 7.4	85.1 ± 12	10.0 ± 5.9	14.8 ± 12

**Table 3**  
Segmentation performance (in percentage) of the five segmentation methods on BUS images with malignant tumors (the best values are in bold).

Methods	ARE (%)	TPVF (%)	FPVF (%)	FNVF (%)
PAORGB	<b>8.2 ± 2.2</b>	<b>88.0 ± 3.7</b>	1.8 ± 0.9	<b>12 ± 3.7</b>
RGB ( $k = 2000, \alpha = 0.02$ )	11.2 ± 0.2	82.8 ± 5.4	1.0 ± 1.6	17.2 ± 5.4
K-means ( $K=3$ )	11.7 ± 4.8	81.7 ± 7.1	<b>1.3 ± 1.0</b>	18.2 ± 7.1
FCM ( $c=3$ )	23.2 ± 17.8	79.3 ± 4.7	5.4 ± 4.2	14.6 ± 5.2
Mad.'s method	14.6 ± 6.7	79.6 ± 9.8	7.0 ± 5.5	20.3 ± 9.8

In the PAORGB, a reference region is required to be marked for the optimization of segmentation results. As the reference region is automatically found, the processes for segmenting the BUS images and extracting lesions of interest can be regarded being automatic. Nevertheless, the step to obtain the TCI (as shown in Fig. 3) requires user's participation which may lead significant influence to the following segmentations. To obtain acceptable segmentations, the operator should be well experienced in examining BUS images and identifying important lesions in clinical practices. In addition, the TCI should be carefully delineated to achieve the full region of the lesion with partial surrounding tissues and the lesion of interest must be locating at the center part. From this point, the proposed PAORGB may be considered as a quasi-automatic segmentation technique. How to automatically extract the TCI from a BUS image and to make the PAORGB a fully segmentation technique will be one of our future studies.

A worth mentioning drawback of the PAORGB is the computation time. As presented in Section 3, averaged computation time of the PAORGB for the TCIs extracted from all of the BUS images much longer than that of the RGB. It is due to the repeated executions of the RGB methods during the process of parameter optimization. For real applications, it may not be suitable as real-time processing is often needed. To overcome this drawback, a high-performance computer with multiple processors should be helpful. In addition, with parallel processing techniques, complex algorithms can be implemented on multiple computing grids, leading to much reduced computation time. We will further make efforts to parallelize the PAORGB method in future work.

In conclusion, this paper proposes a parameter-optimization method which is incorporated into a previously reported segmentation method. The hybrid method is called parameter-automatically optimized robust graph-based segmentation method. The particle swarm optimization algorithm is used to optimize two parameters in a segmentation algorithm (i.e. robust graph-based segmentation method). By taking advantage of Ostu's method, an objective

function is designed for guiding the searching for optimal parameters. The experimental results have shown that the proposed method significantly improves the performance of the RGB and outperforms the other two conventionally used region based methods. It can be expected that the proposed method will be much capable of extracting lesions from BUS images in various clinical practices.

## Acknowledgments

This work is supported by the National Natural Science Foundation of China (Grant Nos: 61125106, 61001181, 91120302, 61072093, 61372007), Natural Science Foundation of Guangdong Province (Grant No.: S2012010009885), the Guangzhou Science and Technology Plan Project (Grant No.: 2012J2200010) and by Shaanxi Key Innovation Team of Science and Technology (Grant No.: 2012KCT-04).

## References

- [1] D.-R. Chen, R.-F. Chang, W.-J. Wu, W.K. Moon, W.-L. Wu, 3-d breast ultrasound segmentation using active contour model, *Ultrasound Med. Biol.* 29 (2003) 1017–1026.
- [2] Y. Wang, D. Tao, X. Gao, X. Li, B. Wang, Mammographic mass segmentation: embedding multiple features in vector-valued level set in ambiguous regions, *Pattern Recognit.* 44 (2011) 1903–1915.
- [3] B. Wang, X. Gao, D. Tao, X. Li, A unified tensor level set for image segmentation, *IEEE Trans. Syst. Man Cybern. Part B: Cybern.* 40 (2010) 857–867.
- [4] X. Gao, B. Wang, D. Tao, X. Li, A relay level set method for automatic image segmentation, *IEEE Trans. Syst. Man Cybern. Part B: Cybern.* 41 (2011) 518–525.
- [5] H. Lu, G. Fang, X. Shao, X. Li, Segmenting human from photo images based on a coarse-to-fine scheme, *IEEE Trans. Syst. Man Cybern. Part B: Cybern.* 42 (2012) 889–899.
- [6] H. Zhou, X. Li, G. Schaefer, M. Emre Celebi, P. Miller, Mean shift based gradient vector flow for image segmentation, *Comput. Vis. Image Underst.* 117 (2013) 1004–1016.
- [7] P. Yan, W. Zhang, B. Turkbey, P.L. Choyke, X. Li, Global structure constrained local shape prior estimation for medical image segmentation, *Comput. Vis. Image Underst.* 117 (2013) 1017–1026.
- [8] Y. Cao, Y. Yuan, X. Li, B. Turkbey, P.L. Choyke, P. Yan, Segmenting images by combining selected atlases on manifold, in: *Medical Image Computing and Computer-Assisted Intervention—MICCAI 2011*, Springer, 2011, pp. 272–279.
- [9] M. Yang, X. Li, B. Turkbey, P. Choyke, P. Yan, Prostate segmentation in MR images using discriminant boundary features, *IEEE Trans. Biomed. Eng.* 60 (2013) 479–488.
- [10] H. Zhou, G. Schaefer, A.H. Sadka, M.E. Celebi, Anisotropic mean shift based fuzzy c-means segmentation of dermoscopy images, *IEEE J. Sel. Top. Signal Process.* 3 (2009) 26–34.
- [11] Y. Xu, T. Nishimura, Segmentation of breast lesions in ultrasound images using spatial fuzzy clustering and structure tensors, *World Acad. Sci. Eng. Technol.* 53 (2009).
- [12] Y.-L. Huang, D.-R. Chen, Automatic contouring for breast tumors in 2-d sonography, in: *Engineering in Medicine and Biology Society, 27th Annual International Conference of the IEEE-EMBS 2005*, 2005, IEEE, pp. 3225–3228.
- [13] A. Madabhushi, D.N. Metaxas, Combining low-, high-level and empirical domain knowledge for automated segmentation of ultrasonic breast lesions, *IEEE Trans. Med. Imaging* 22 (2003) 155–169.
- [14] Q.-H. Huang, S.-Y. Lee, L.-Z. Liu, M.-H. Lu, L.-W. Jin, A.-H. Li, A robust graph-based segmentation method for breast tumors in ultrasound images, *Ultrasonics* 52 (2012) 266–275.
- [15] J. Shi, Z. Xiao, S. Zhou, Automatic segmentation of breast tumor in ultrasound image with simplified PCNN and improved fuzzy mutual information, in: *Proceedings of the SPIE*, vol. 7744, pp. 77441P-1.
- [16] P.F. Felzenszwalb, D.P. Huttenlocher, Efficient graph-based image segmentation, *Int. J. Comput. Vis.* 59 (2004) 167–181.
- [17] C.T. Zahn, Graph-theoretical methods for detecting and describing gestalt clusters, *IEEE Trans. Comput.* 100 (1971) 68–86.
- [18] L. Davis, *Genetic Algorithms and Simulated Annealing*, Morgan Kaufman Publishers, Inc., Los Altos, CA, 1987.
- [19] M. Gang, Z. Wei, C. Xiaolin, A novel particle swarm optimization algorithm based on particle migration, *Appl. Math. Comput.* 218 (2012) 6620–6626.
- [20] R. Storn, K. Price, Differential evolution—a simple and efficient heuristic for global optimization over continuous spaces, *J. Glob. Optim.* 11 (1997) 341–359.
- [21] D.A.V. Veldhuizen, G.B. Lamont, Multiobjective evolutionary algorithms: analyzing the state-of-the-art, *Evol. Comput.* 8 (2000) 125–147.
- [22] Q.-H. Huang, Discovery of time-inconsecutive co-movement patterns of foreign currencies using an evolutionary biclustering method, *Appl. Math. Comput.* 218 (2011) 4353–4364.
- [23] Q. Huang, D. Tao, X. Li, A. Liew, Parallelized evolutionary learning for detection of biclusters in gene expression data, *IEEE/ACM Trans. Comput. Biol. Bioinformatics* 9 (2012) 560–570.
- [24] J.A. Noble, D. Boukerroui, Ultrasound image segmentation: a survey, *IEEE Trans. Med. Imaging* 25 (2006) 987–1010.
- [25] M. Elad, On the origin of the bilateral filter and ways to improve it, *IEEE Trans. Image Process.* 11 (2002) 1141–1151.
- [26] N. Otsu, A threshold selection method from gray-level histograms, *Automatica* 11 (1975) 23–27.



**Qinghua Huang** received B.E. and M.E. degrees in automatic control and pattern recognition, both from the University of Science and Technology of China, China, in 1999 and 2002, respectively. He received Ph. D. degree in biomedical engineering in 2007 from the Hong Kong Polytechnic University, Hong Kong. Since 2008, he has been an associate professor in the School of Electronic and Information Engineering, South China University of Technology, China. His research interests include ultrasonic imaging, medical image analysis, bioinformatics, intelligent computation and its applications.



**Xiao Bai** received the B.E. degree in computer science from Beihang University of China, Beijing, China, in 2001, and the Ph.D. degree from the University of York, York, U.K., in 2006. He was a research officer (fellow, scientist) in the Computer Science Department, University of Bath, until 2008. He is currently an associate professor in the School of Computer Science and Engineering, Beihang University. He has published more than forty papers in journals and refereed conferences. His current research interests include pattern recognition, image processing and remote sensing image analysis.



**Yingguang Li** received the B.E. and M.E. degrees in information engineering at South China University of Technology, China, in 2010, and 2013, respectively. His research interests include biomedical engineering and pattern recognition.



**Lianwen Jin** received a B.S. degree from the University of Science and Technology of China and a Ph.D. degree from the South China University of Technology in 1991 and 1996, respectively. He is currently a professor at the School of Electronic and Information Engineering, South China University of Technology. His research interests include character recognition, pattern analysis and recognition, image processing, machine learning and intelligent systems. He has published more than 100 scientific papers.

**Xuelong Li** is a full professor with the Center for OPTical IMagery Analysis and Learning (OPTIMAL), State Key Laboratory of Transient Optics and Photonics, Xi'an Institute of Optics and Precision Mechanics, Chinese Academy of Sciences, Xi'an 710119, Shaanxi, P.R. China.